Supporting Information

Vertically Aligned MoS_2 on Ti_3C_2 (MXene) as an Improved HER Catalyst

Nuwan H. Attanayake,[1,2] Sasitha C. Abeyweera,[1] Akila C. Thenuwara,[1,2] Babak Anasori,[3] Yury Gogotsi,[3] Yugang Sun,[1] Daniel R. Strongin.[1,2]

[1] Department of Chemistry, Temple University, 1901 N. 13th Street, Philadelphia, PA 19122 (USA)

[2] Center for Computational Design of Functional Layered Materials (CCDM)

[3] Department of Materials Science and Engineering, and A.J. Drexel Nanomaterials Institute, Drexel University, Philadelphia, PA 19104 (USA)

Table of contents **Page**

Experimental Section

Chemicals

All chemicals were analytical grade or technical grade and were used as received from the supplier (Fischer, Alfa Aesar and Sigma Aldrich) without further purification.

Synthesis of Ti_3C_2

Synthesis of the Ti_3AlC_2 MAX phase has been described previously.[1] Ti_3C_2 MXene powder was prepared by the following etching procedure. One gram of Ti_3AlC_2 powder was slowly added into a solution composed of 1 g lithium fluoride (LiF, Alfa Aesar, 98+ %) in 20 ml 9 M hydrochloric acid (HCl, Fisher, technical grade, 35-38%). This addition was followed by stirring at 35 °C for 24 h. The acidic suspension was washed with 100 ml of deionized (DI) water and centrifuged until a pH ≥ 6 was reached and a stable dark green supernatant of Ti_3C_2 was collected after 30 min centrifugation at 3500 rpm. The resulting Ti_3C_2 supernatant solution was filtered using a vacuum-assisted filtration through a polypropylene filter (3501 Coated PP, Celgard LLC, Charlotte, NC), followed by drying at room temperature under vacuum.

Synthesis of the IE-MoS_2 and IE-MoS_2/Ti_3C_2 at different growth temperatures

The synthesis of the IE-MoS_2 was similar to the procedure developed by Sun Y. et al..[2] In brief 10 mg of $(NH_4)_2MoS_4$ (Alfa Aesar, 99.95%) was dispersed in 6 mL of DMF (Sigma Aldrich, ≥99.8%). The mixture was stirred with the assistance of a magnetic stirrer at ambient conditions for 30 min to uniformly disperse the $(NH_4)_2MoS_4$. The solution was then heated in a sealed vessel in a microwave (Monowave 300, Anton Parr) at the desired temperature for 2 h. The reaction vessel was quickly cooled to room temperature with a pressurized air flow. The product obtained was collected by centrifugation at 10000 rpm for 5 min, then washed with DI water followed by washing three times with a acetone/ethanol (1:1) mixture. The sample was dried in an oven overnight at 60 ^{0}C. In the case of the $MoS_2 \perp Ti_3C_2$ synthesis, the Ti_3C_2 (5 mg) was initially sonicated in the DMF for 1 h before adding $(NH_4)_2MoS_4$ (10 mg). The resulting mixture

was stirred with the assistance of magnetic stirring for a further 30 min. Thereafter the procedure was similar to the synthesis of IE-MoS_2.

Characterization

Samples for SEM were prepared by drop casting the sample of interest in a mixture of water/ethanol (4:1) on to a silicon wafer. SEM images were obtained with a FEG Quanta 450 FEG electron Microscope, operated at an acceleration voltage of 20 kV. Energy Dispersive X-ray Spectra (EDS) were obtained with an X-Max^N 50 spectrometer (Oxford Instrument) mounted on the SEM. Samples for TEM were obtained by diluting the above samples with ethanol and drop casting them onto holey carbon grids. TEM and HRTEM images were recorded with a JEOL JEM-1400 microscope and JEOL JEM-2100 respectively. Raman measurements were performed using a Horiba Jobin Yvon Labram HR800 Evolution confocal Raman spectrometer with 532 nm laser excitation, Olympus MPlan N 100x microscope objective that focused excitation light to an ~1μm spot, and a 1800 gmm grating providing ~2 cm^{-1} spectral resolution. Samples were drop cast onto a silicon wafer for Raman spectroscopy and dried in air overnight before collecting the spectra.

Electrochemical characterization

Electrocatalytic were performed in an acidic media (0.5 M H_2SO_4) that was degassed by bubbling N_2 (for 20 min), using a CHI 660E potentiostat. The potentiostat operated in a standard three-electrode configuration at ambient temperature (20 ± 2 °C). All the potentials were measured with respect to a standard calomel reference electrode (CH instruments) and a Pt wire as the counter electrode. 5 μL of a catalyst ink suspension was drop cast on to a 3 mm diameter glassy carbon electrode (loading 50 μg) which was used as the working electrode. The electrode

was dried in a fume hood for 30 min. The ink solution was prepared by adding 5 mg of the catalyst to 0.5 mL of an ethanol/DI water mixture (1:3), that was sonicated for 1 h. It should be noted that no binder (e.g. Nafion) was added when the catalyst ink was prepared. All the polarization curves were recorded at 10 mV/s scan rate after correcting for any iR losses. iR loses in the solution was determined to be (8-10 Ω) by a CHI 660E potentiostat via the resistance test, which were then corrected from the polarization curves by subtracting iR (current x resitance) from the potential (V) . Polarization curves obtained with graphite rod counter electrode are given in SI figure 9. For all the catalysts tested here, polarization curves were replicated 3 times and obtained after cycling for 30 cycles. The onset potential, overpotential and Tafel slopes reported in this work are based on an analysis of these data. Chronopotentiometry measurements of each sample were carried out at a current density of 10 mA/cm^2_{geo} for 20 h in 0.5 M H_2SO_4 without any corrections for iR loses. Electrochemical Impedance Spectroscopy (EIS) Nyquist plots were obtained at 170 mV overpotential within the frequency range 0.1 Hz to 10^6 Hz. Cyclic voltamograms obtained at various scan rates (20, 40, 60, 80, 100, 120, 140 mVs^{-1}) in the potential range 180-280 mV vs SCE were used to determine the ECSA and double layer capacitance. Electrochemical impedance spectroscopy was used to obtain Mott-Schottky plots. Experiments were carried out in 0.1 M Na_2SO_4 solution (pH 7.2) at 100, 1000, and 10000 Hz.

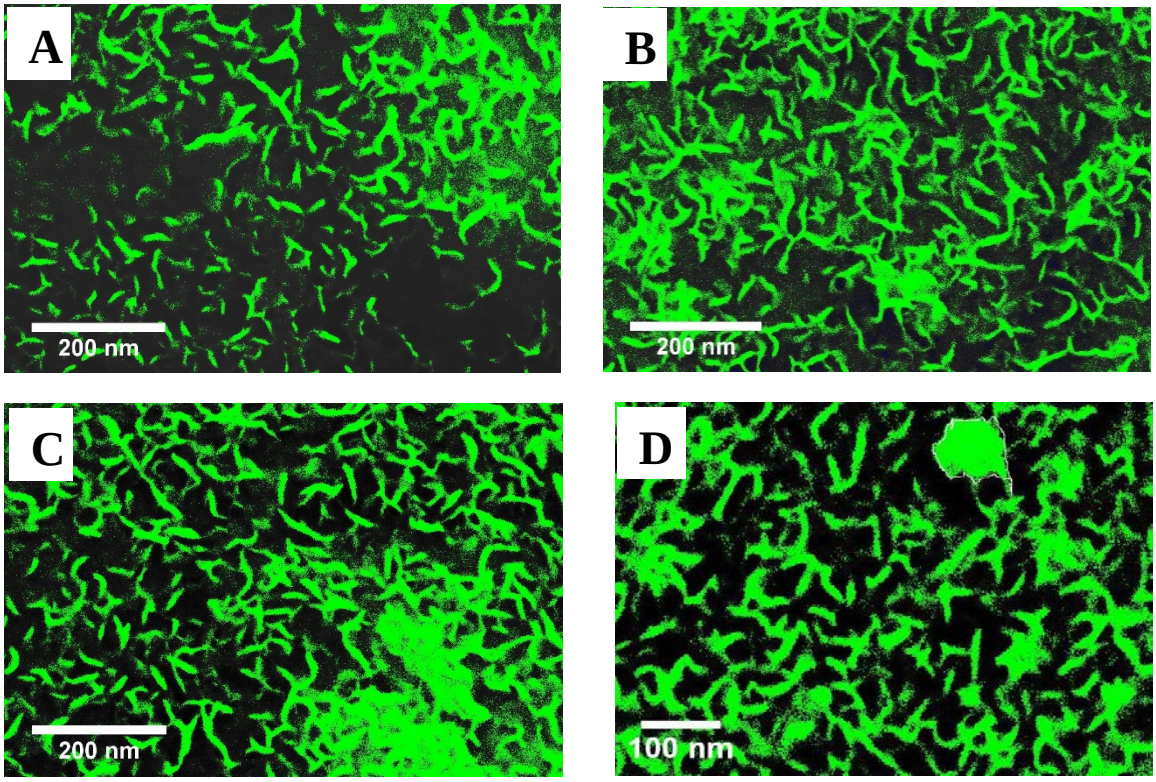

Figure S1: Contrast profiles obtained from Imagej varying the threshold of the SEM images. These images were used to obtain the edge density given in table S1 for IE-$MoS_2 \perp Ti_3C_2$ at growth temperatures of A) 200, B) 220, C) 240 and D) 260 ^{0}C. In the calculation of vertically aligned edges, the area from flower like morphologies (marked by the white line) have been subtracted from image D.

Table S1: Edge density of IE-MoS_2 grown on Ti_3C_2. The area with the green pixels were normalized to the total area of the image to obtain the density.

Image	Temperature (^{0}C)	Edge density (%)
A	**200**	**27.6**
B	**220**	**33.1**
C	**240**	**36.1**
D	**260**	**34.3**

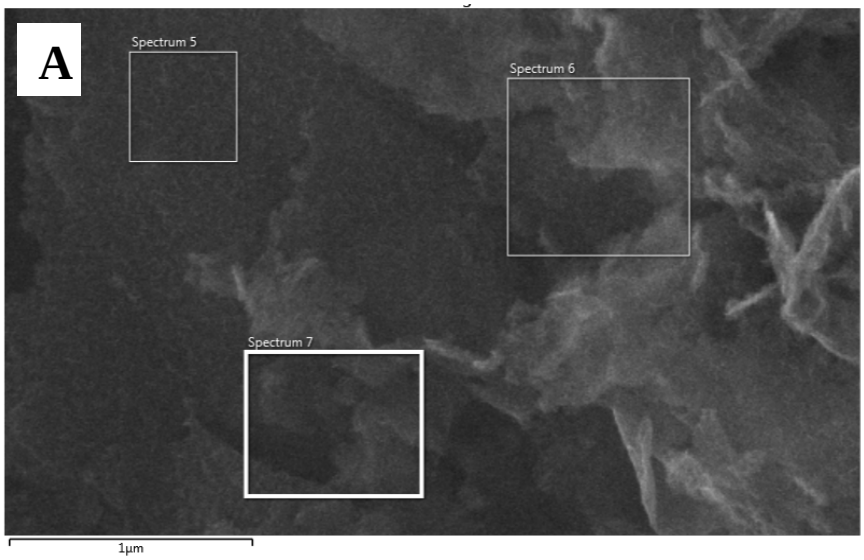

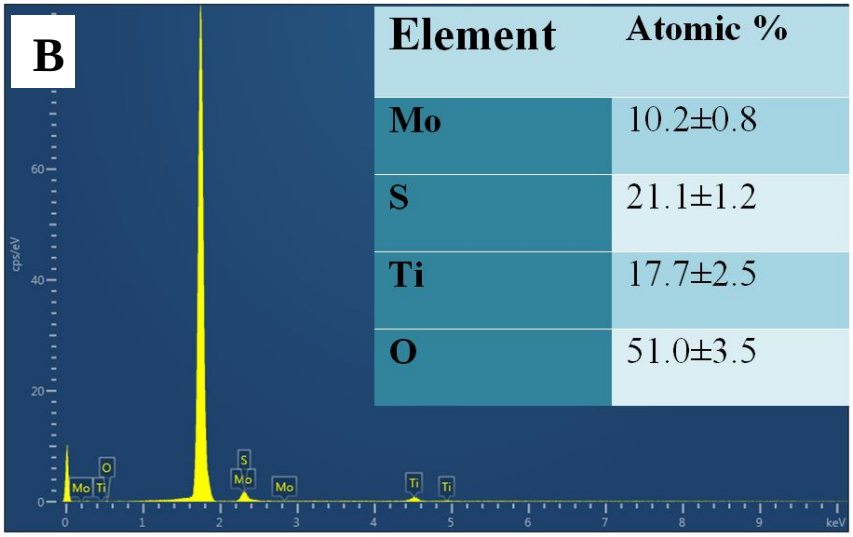

Figure S2: A) SEM micrograph of IE-$MoS_2 \perp Ti_3C_2$@240 showing three regions used for quantifying the atomic percentages of Ti, Mo and S with EDS, B) Intensity maps of the EDS spectra for different Ti, Mo and S (inset: average atomic percentage of each component).

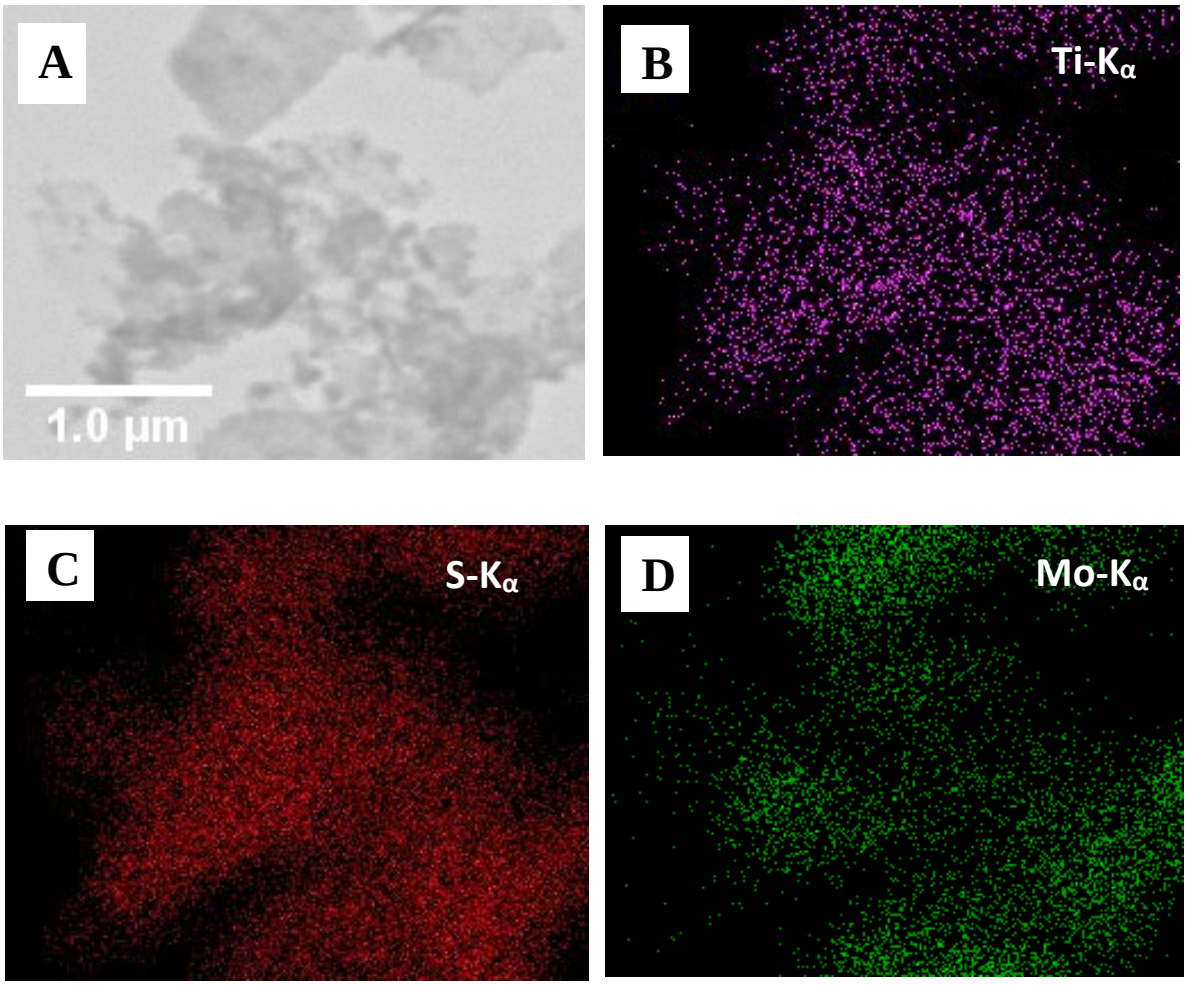

Figure S3: A) STEM image and B), C) and D)STEM-EDS maps of the elemental composition of the IE-$MoS_2 \perp Ti_3C_2$@240.

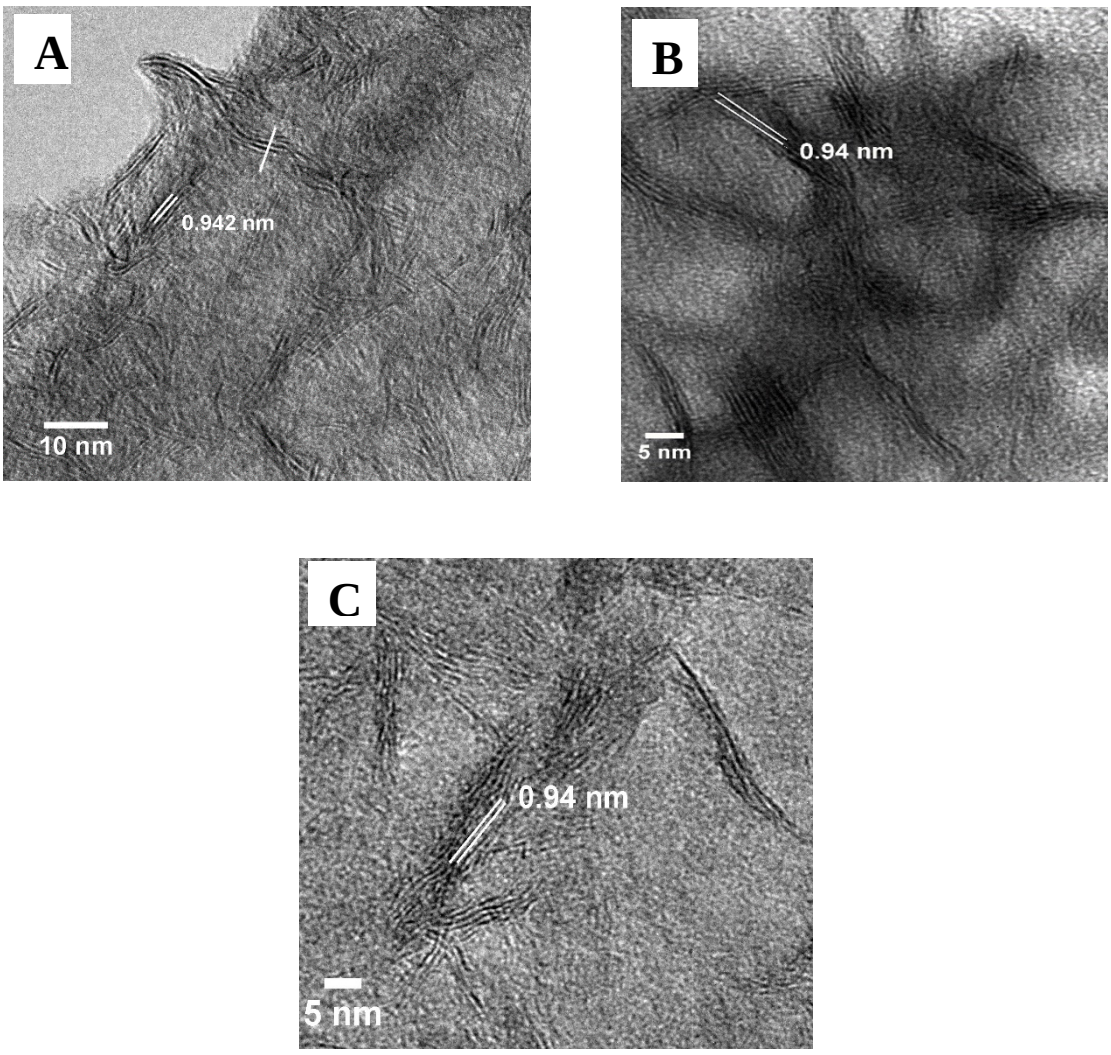

Figure S4: A), B) and C) HRTEM images of $MoS_2 \perp Ti_3C_2$ for samples grown at a) 200, b) 220 and c) 260 ^{0}C. These images show that the interlayer spacing of each is ~ 0.94 nm irrespective of the temperature of synthesis.

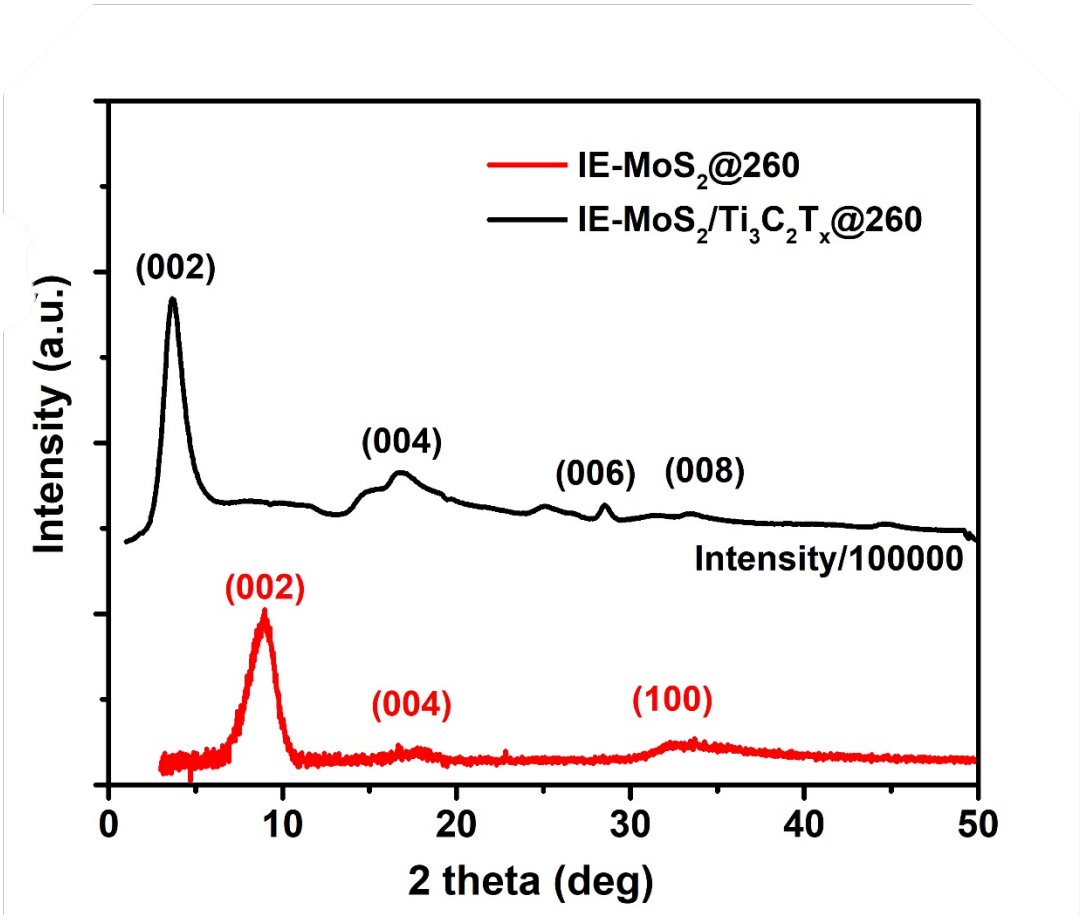

Figure S5: XRD diffractogram for IE-MoS_2⊥Ti_3C_2@260 (black) normalized by dividing by a factor of 100000. The relatively weak (002) at 9.4^0, (004) at 18.8^0 and (100) at 32.2^0 Bragg reflection peak of MoS_2 (red) of interlayer expanded MoS_2 is not seen in this diffractogram of IE-MoS_2/Ti_3C_2@260 due to the masking of the peaks by the more intense peaks of the MXene.

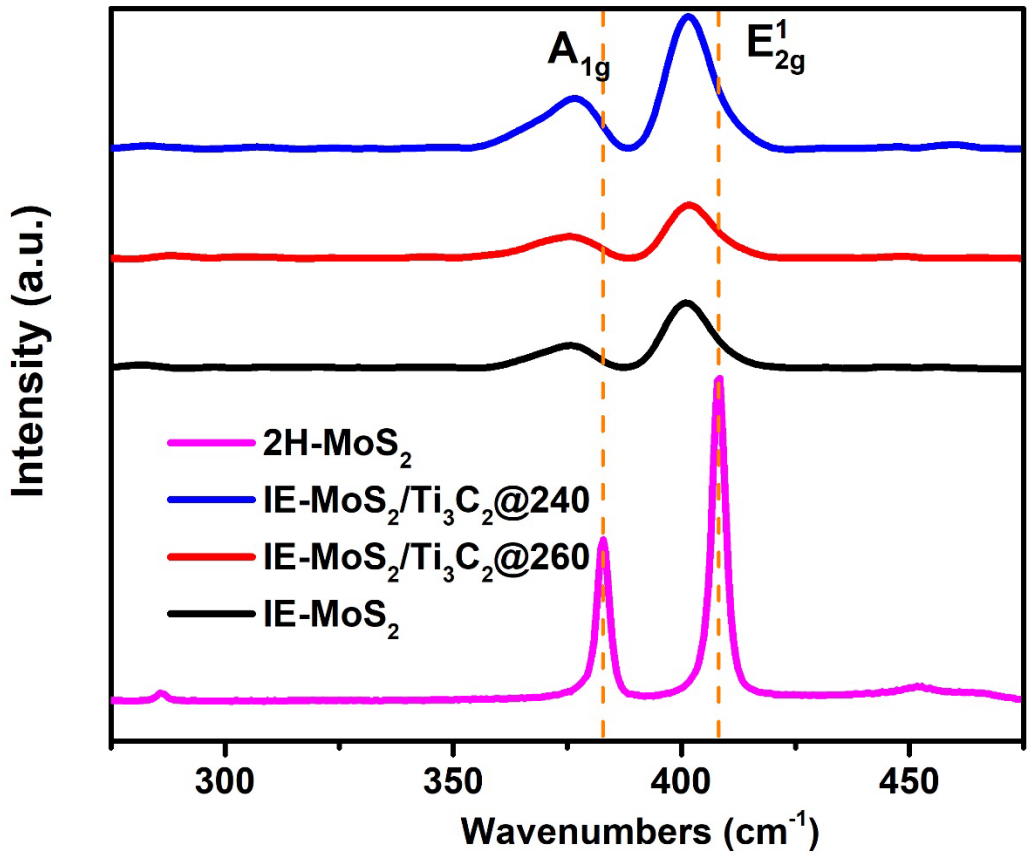

Figure S6: Comparison of the Raman spectra of IE-MoS_2 and the heterostructures synthesized at 240 and 260 ^{0}C. A blue shift is observed in the IE-MoS_2 and heterostructures relative to commercial 2H-MoS_2.

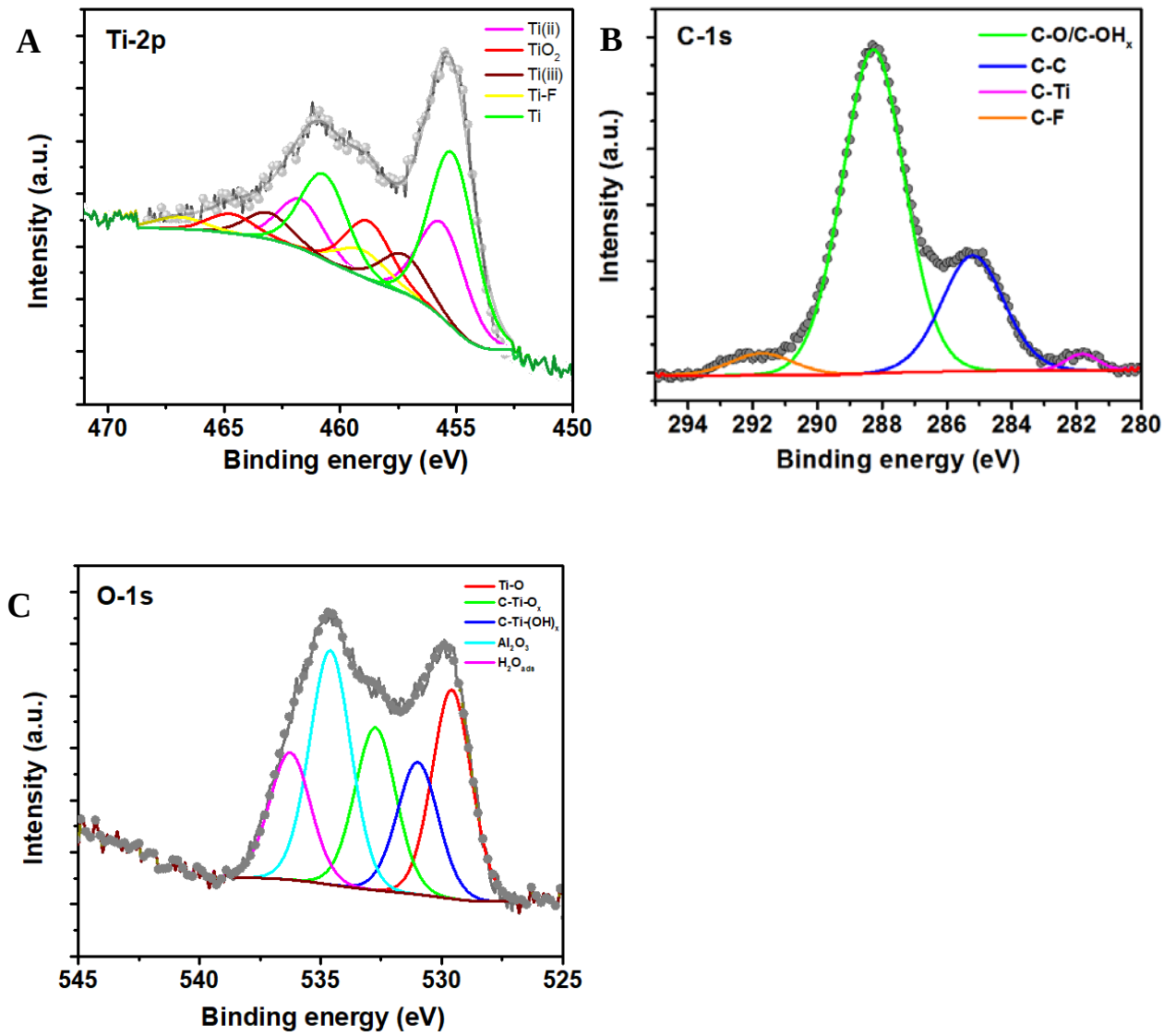

Figure S7: XPS spectra for the A) Ti 2p, B) C 1s, and C) O 1s region for Ti_3C_2 before nucleating MoS_2.

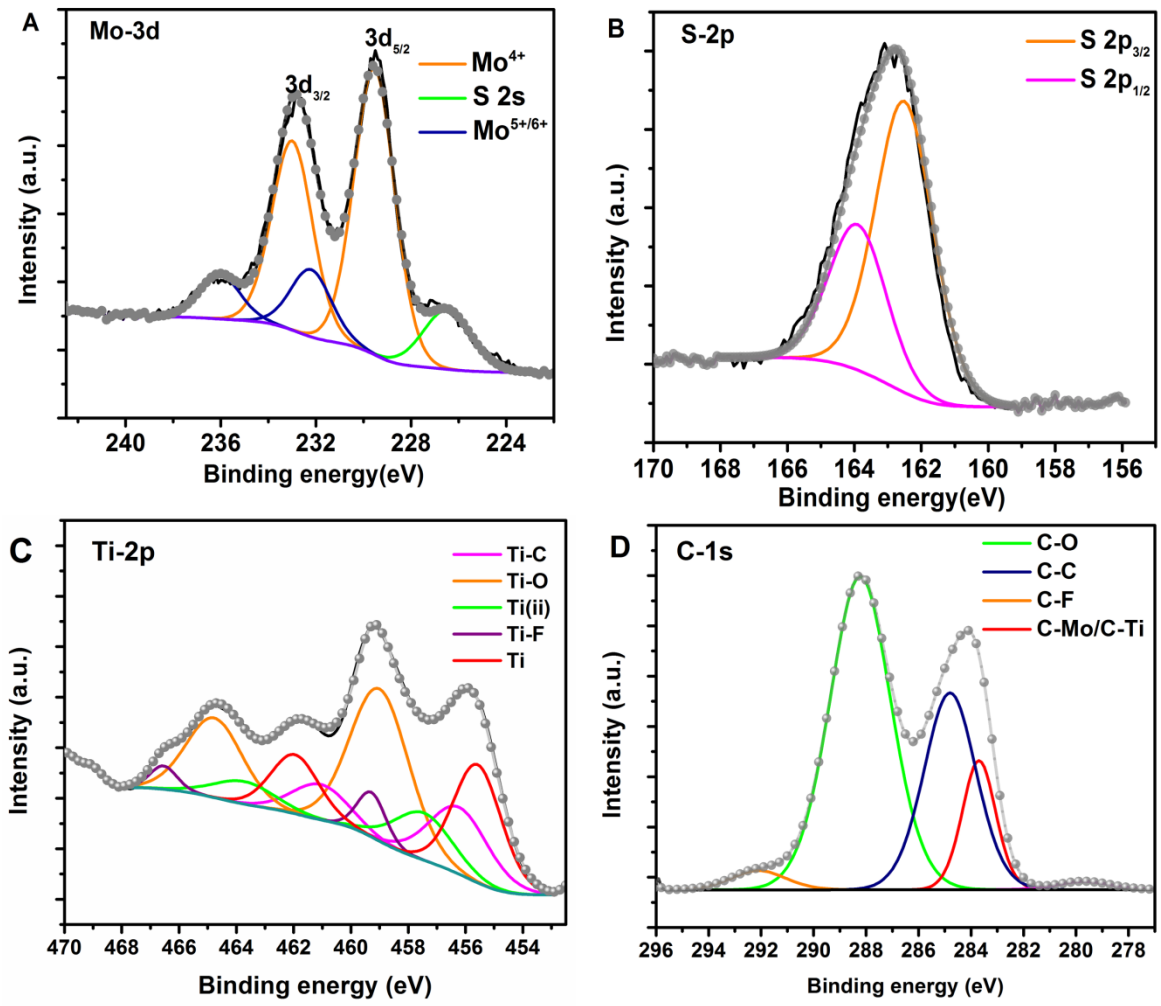

Figure S8: XPS for the A) Mo-3d, B) S-2p, C) Ti-2p and D) C-1s region for IE-$MoS_2 \perp Ti_3C_2$@240 ^{0}C.

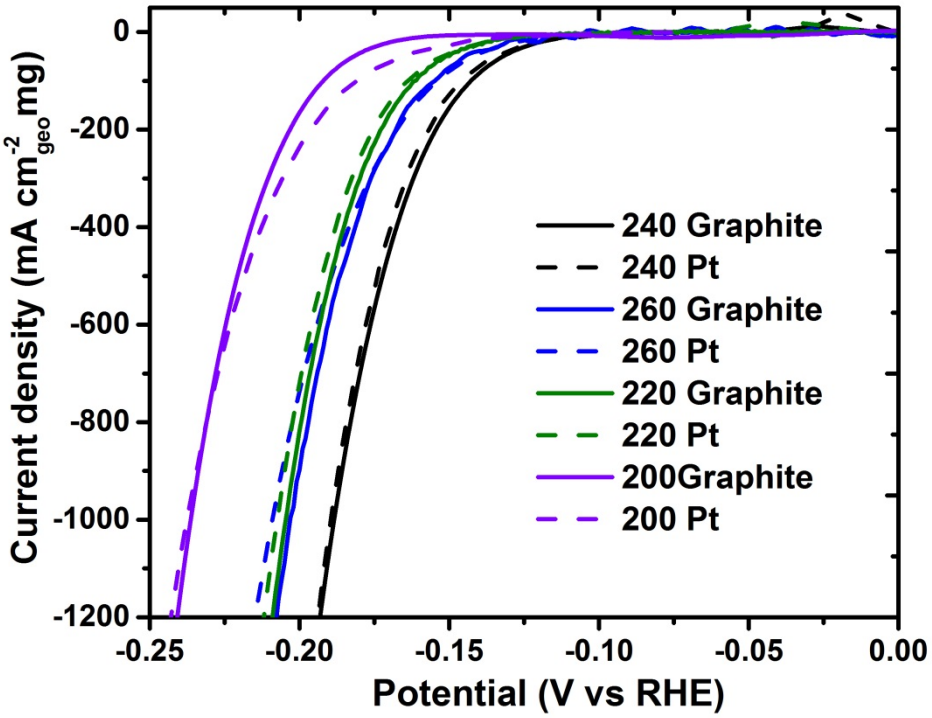

Figure S9: Polarization plots obtained after cycling for 1000 cycles in 0.5 M H_2SO_4 with a Pt counter electrode and a graphite rod counter electrode. These LSV curves are almost identical to each other implying there had not been an influence of the counter electrode used.

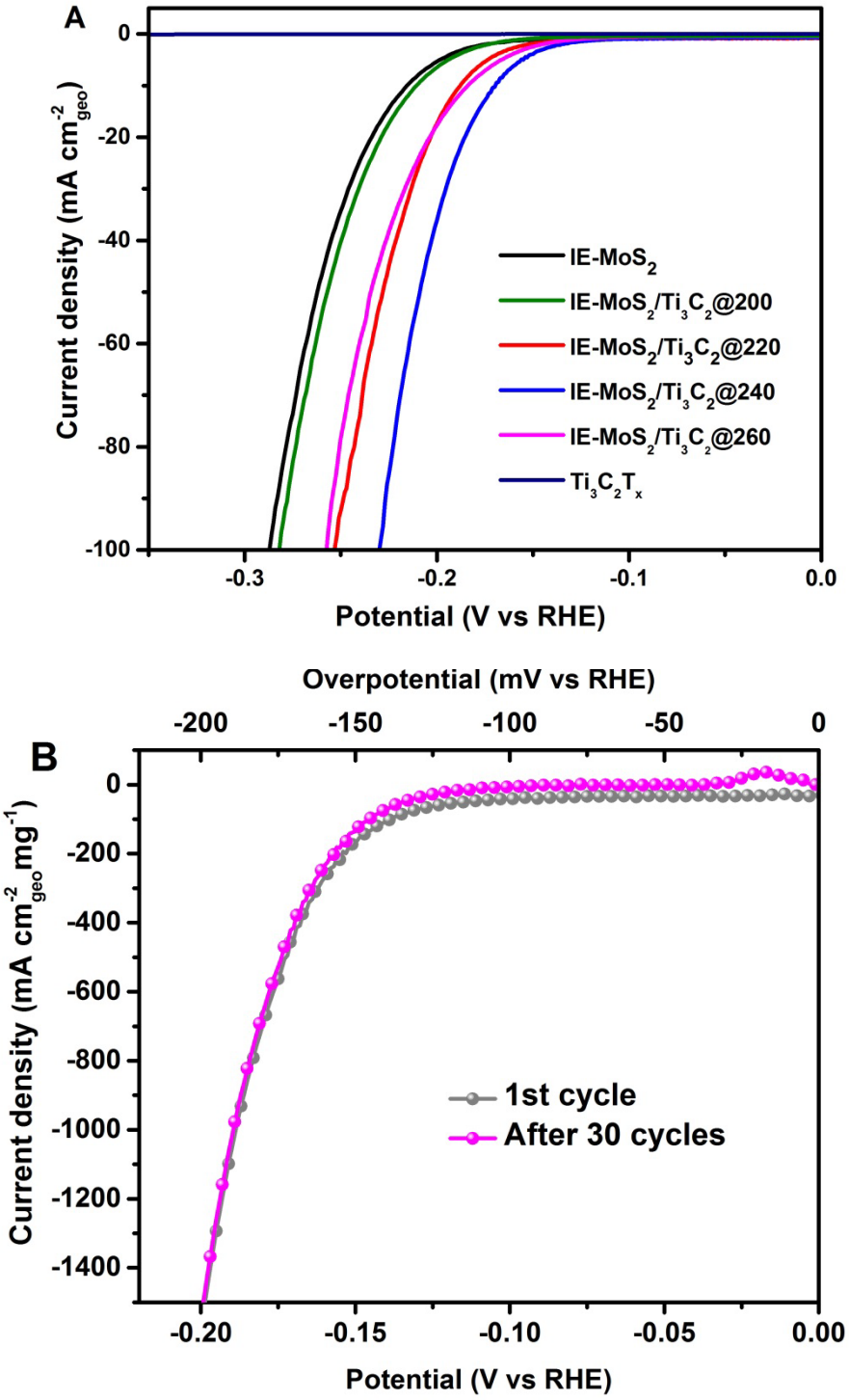

Figure S10: A) Polarization plot normalized to geometric surface area of the electrode. The MXene alone shows a high overpotential of ~500 mV @ 10 mA/cm^2. B) Polarization plot of IE-MoS_2⊥Ti_3C_2@240 ^{0}C for the first and 30th cycle. The cycling reduced capacitive background currents in the polarization curves.

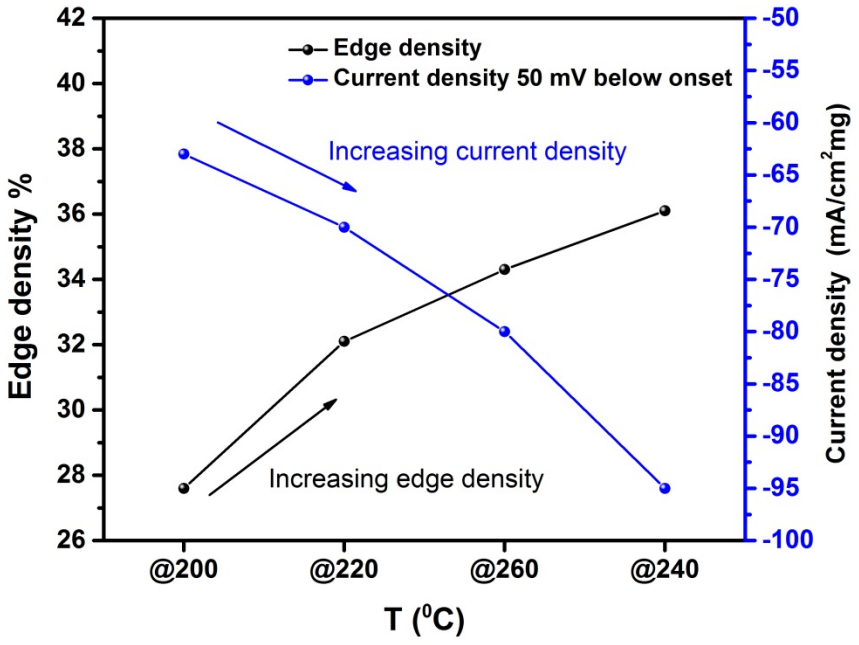

Figure S11: Comparison of current density (50 mV below the onset) and edge density of samples prepared at different temperatures. The current density increases with the increasing edge density of MoS_2 on the Ti_3C_2 MXene.

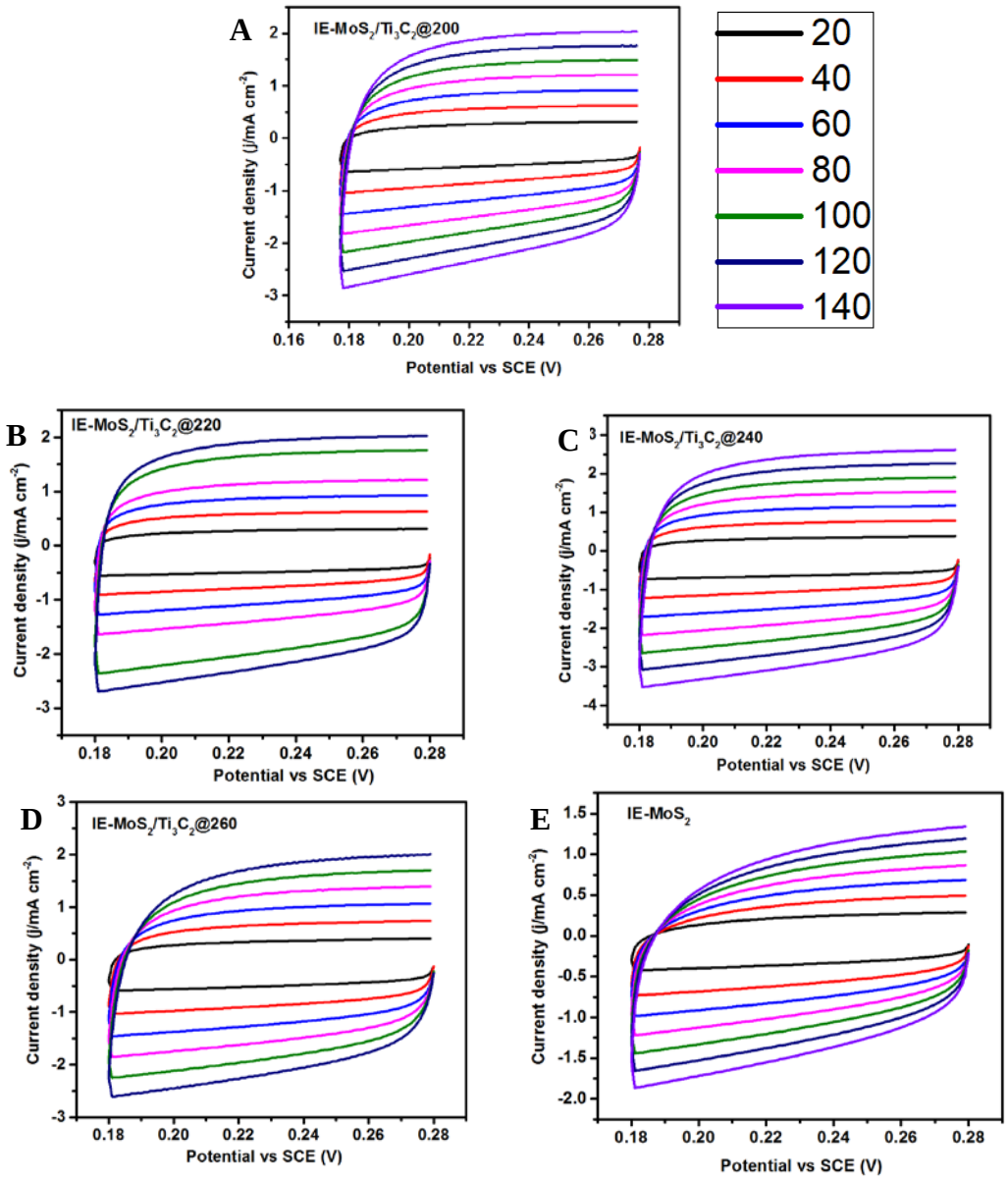

Figure S12 : Cyclic voltammetry (CV) curves obtained in 0.5 M H_2SO_4 from 180 to 280 mV vs SCE to investigate the capacitive currents used to calculate the electrochemically active surface area of the catalysts synthesized at different temperatures. The legend on the top right corner gives the scan rates (20, 40, 60, 80, 100, 120 and 140 mV/s). The presence of rectangular CVs implies the currents are non-faradaic and are capacitive.

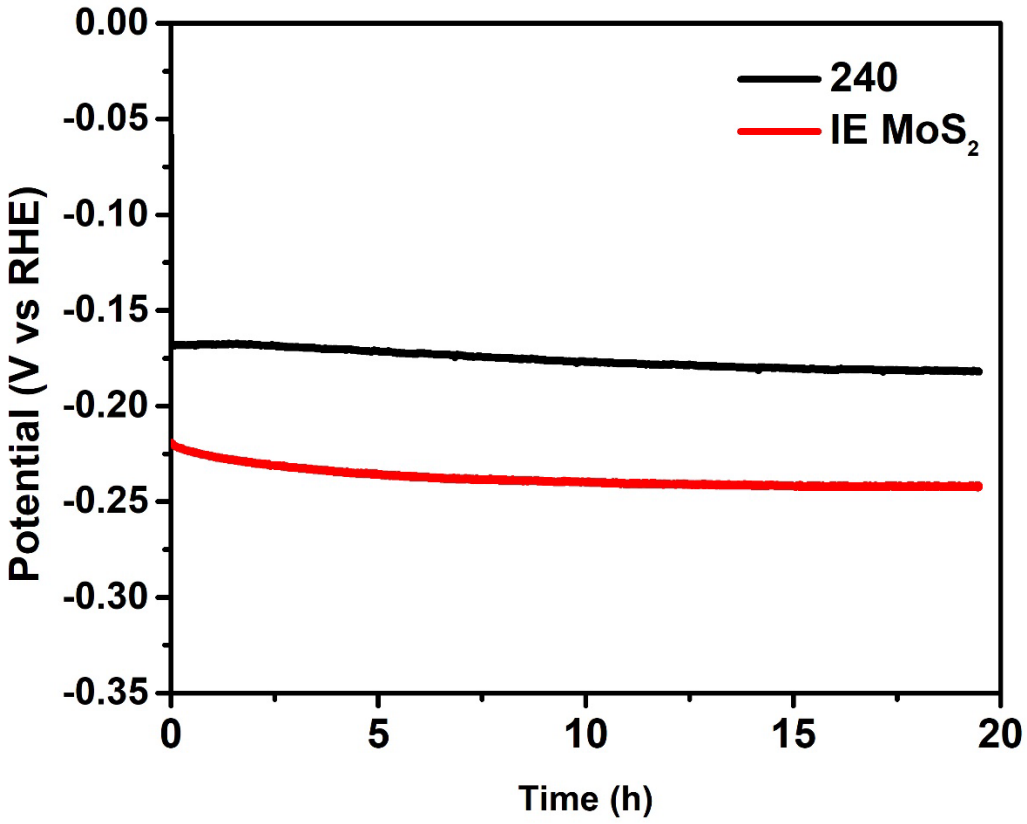

Figure S13: Chronopotentiometry at 10 mA/cm^2_{geo} of the IE-MoS_2 and the heterostructure synthesized at 240 ^0C over a period of 20 h in 0.5 M H_2SO_4. The catalysts show good stability in the region in the time period the tests were carried out with less than 7% decrease in potential to maintain a constant current of 10 mA/cm^2_{geo}.

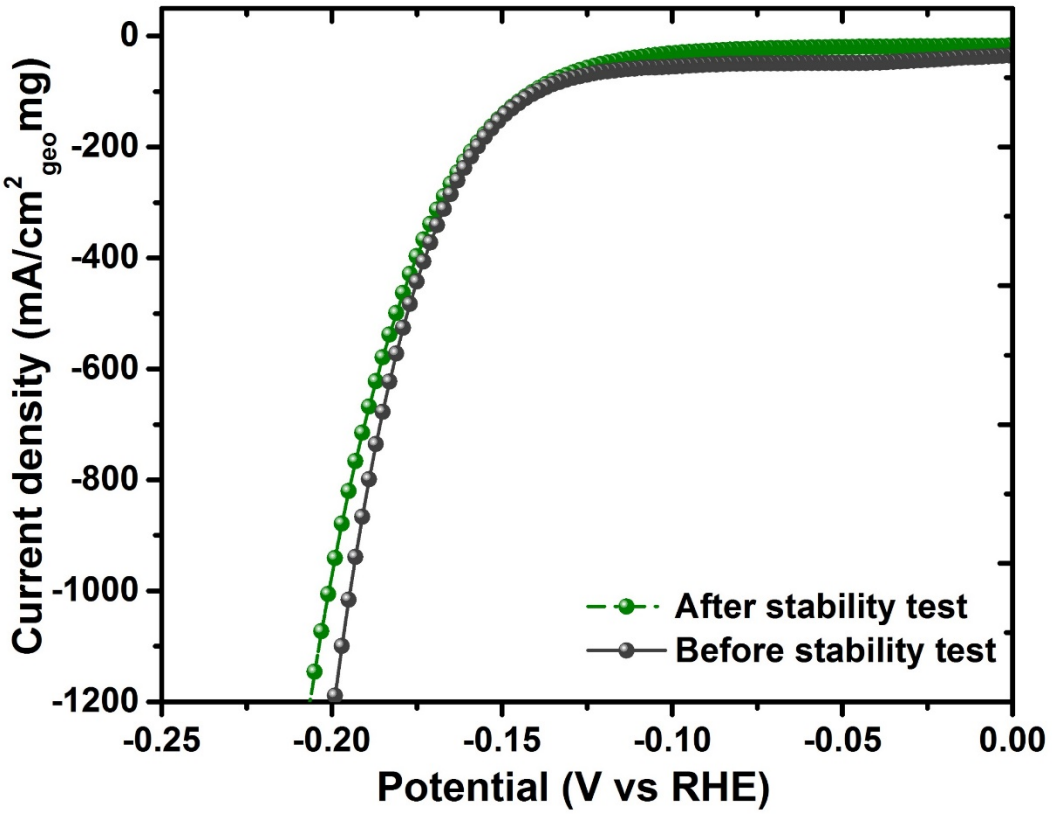

Figure S14: Polarization plots obtained before and after the stability (chronopotentiometry) test for IE-$MoS_2 \perp Ti_3C_2$@240 ^{0}C.

The Mott-Schottky plots of IE-$MoS_2 \perp Ti_3C_2$@T where T is 200, 220, 240 and 260 ^{0}C were obtained in 0.1 M Na_2SO_4 vs a Ag/ AgCl reference electrode (Figure 5a). From the Mott-Schottky relation:

$$\frac{1}{{C_{SCL}}^2} = \frac{2}{e \in\in_0 N_D}\left(E - E_{FB} - \frac{kT}{e}\right)$$

Where C_{SCL}-capacitance of the space charge layer, e is the charge of an electron, $\in_0$ is permittivity of free space 8.85×10^{-12} F m^{-1} , $\in$ is dielectric constant of MoS_2, E is applied potential, E_{FB} is flatband potential, N_D is donor density, k is Boltzmann constant, T is Kelvin temperature.[3-5]

Table S2: Carrier concentration of MoS_2 grown on Ti_3C_2

Samples	Carrier concentration (cm^{-3})
IE-$MoS_2 \perp Ti_3C_2$@200	1.1785×10^{20}
IE-$MoS_2 \perp Ti_3C_2$@220	2.2701×10^{20}
IE-$MoS_2 \perp Ti_3C_2$@240	2.5996×10^{20}
IE-$MoS_2 \perp Ti_3C_2$@260	6.3213×10^{20}

References

1. M. Alhabeb, K. Maleski, B. Anasori, P. Lelyukh, L. Clark, S. Sin and Y. Gogotsi, *Chem. Mater.*, 2017, **29**, 7633-7644.
2. M.-R. Gao, M. K. Y. Chan and Y. Sun, *Nat. Commun.*, 2015, **6**, 7493.
3. Y. Cong, H. S. Park, S. Wang, H. X. Dang, F.-R. F. Fan, C. B. Mullins and A. J. Bard, *J. Phys. Chem. C*, 2012, **116**, 14541-14550.
4. T. Kirchartz, W. Gong, S. A. Hawks, T. Agostinelli, R. C. I. MacKenzie, Y. Yang and J. Nelson, *J. Phys. Chem. C*, 2012, **116**, 7672-7680.
5. W. J. Basirun, M. Sookhakian, S. Baradaran, Z. Endut, M. R. Mahmoudian, M. Ebadi, R. Yousefi, H. Ghadimi and S. Ahmed, *Sci. Rep.*, 2015, **5**, 9108.